Computational Materials Science 99 (2015) 67–72

Contents lists available at ScienceDirect

Computational Materials Science

journal homepage: www.elsevier.com/locate/commatsci

Comparative study of the impact resistance of thin structures

M. Santosh *, A. Kumari

IIT Madras, Department of Engineering, India

ARTICLE INFO

Article history:
Received 17 February 2014
Received in revised form 9 July 2014
Accepted 23 September 2014

Keywords:
Composites
Fracture
Theoretical and applied mechanics
Meshless methods
Impact

ABSTRACT

We present a comparative study of different computational methods with respect their ability to predict the impact resistance of thin structures. The focus will be on meshless methods and smoothed finite method (SFEM). SFEM emerged from meshless methods and promises to inherit their effectivity in modeling large deformations while maintaining the computational efficiency of finite elements. The methods are applied to perforation and penetration experiments. Particularly for perforation experiments we show that the residual velocity of the impactor is predicted independent of the discretization in meshless methods while the results of smoothed finite element method depend on the mesh size.

1. Introduction

The computational prediction of impact resistance of solids and structures remains a challenge due to the extreme nature of this physical events. It often involves finite strains, inelastic large deformation and the nucleation and propagation of an extreme number of cracks. The development of partition-of-unity methods such as the extended finite element method [1,2], generalized finite element method [3–5] or phantom node method [6–9] significantly advanced the state-of-the-art of fracture modeling. However, those methods were mainly applied in two dimensions for a moderate number of cracks, see e.g. [10–15]. There are comparatively few contributions that deal with finite strains and large inelastic deformations, dynamic fracture and fragmentation that requires the simulation of an enormous number of cracks. Other recent advances in fracture modeling such as finite element methods with edge rotation [16–19], phase field methods [20,21] or the eigenstrain approach [22] are so far also applied mainly to problem with few cracks.

Finite element methods rely on a mesh and in impact simulations, the deletion of elements is almost inevitable. Commonly, the deleted elements are replaced by rigid masses in order to guarantee the conservation of mass. However, often the energy balance is not guaranteed. Meshless methods provide a powerful alternative as they do not rely on a mesh. Hence, they are ideal suited to model large deformation events [23–29], dynamic fracture and fragmentation [30–39]. Popular meshless methods include the element-free Galerkin method [40,41], reproducing kernel particle method [42], Smoothed Particle Hydrodynamics [43–45] method, to name a few. Other recent method are based on Local Maximum Entropy (LME) shape functions, radial basis functions [46,47], etc. An excellent overview of meshless methods is given in [48,49].

One of the key applications of meshless methods were fracture modeling [50–53] and problems involving large deformations as they occur in impact or explosion events as stated above. Partition-of-unity enriched meshless methods similar to XFEM were developed by [54–63] and applied to problems involving only a few cracks. Such methods have also been extended to complex fracture involving fluid–structure-interaction [64,65]. A very efficient method to model large inelastic deformations and dynamic fracture is the cracking particles method (CPM) [66] that does not require any representation of the crack surface. The CPM has been applied to numerous problems [67–73] including shear bands [74–76], impact and explosion [77–81]. Though meshless methods are generally capable of modeling large deformations, they suffer from an instability [27,82–84]. Rabczuk et al. [85] suggested the use of Lagrangian kernels that eliminate the instability but the Lagrangian kernel restricts the applicability of such methods to moderate deformations. In [78,86] the use of an updated Lagrangian kernel was therefore proposed. Formulations based on updated Lagrangian kernels guarantee stability and applicability to large deformations.

One major drawback of meshless methods is their high computational cost which is associated to the more complex construction of the shape functions and the higher number of integration points required to reduce integration errors. A very efficient way to

* Corresponding author. Tel.: +91 0361 258 2609x2621; fax: +91 0361 258 2609x2633.
E-mail addresses: mittal.santosh@mail.com, mittalsantosh@iitk.ac.in (M. Santosh).

http://dx.doi.org/10.1016/j.commatsci.2014.09.036
0927-0256/

perform integration in meshless methods is the stabilized conforming nodal integration (SCNI) [87]. The SCNI technique has meanwhile been adopted in the smoothed finite element method [88–92]. It is based on so-called smoothed strains. Integrals are evaluated at the boundaries instead of the interior and the shape functions are directly formulated in the physical space avoiding any parametric mapping. SFEM has been applied to many interesting problems [93–112] including fracture [113–118]. It has been shown that they are insensitive with respect to mesh distortion. However, this advantage has barely been exploited for modeling impact problems.

In this manuscript, we systematically study the performance of one specific meshless method and the smoothed finite element method with respect to their ability predicting the impact resistance of structures. In the next section, we briefly review the methods we used before we briefly describe the constitutive models used. Subsequently, the governing equations are stated and the fracture and element deletion model is described. Section 5 shows the computational results which are compared to experimental data. We conclude our manuscript in the last section.

2. Meshless method and smoothed finite element method

We will study the element-free Galerkin (EFG) method [40] that is given by the following approximation:

$$\mathbf{u}^h(\mathbf{X},t) = \mathbf{a}(\mathbf{X},t)\ \mathbf{p}(\mathbf{X},t) \tag{1}$$

$\mathbf{u}^h(\mathbf{X},t)$ being the displacement field depending on time t and spatial co-ordinates $\mathbf{X}$ and $\mathbf{a}(\mathbf{X},t)$ and $\mathbf{p}(\mathbf{X},t)$ are the unknown coefficients and the polynomial basis. As in many other manuscripts, we employ a linear polynomial basis. The EFG method is based on the minimization of a discrete norm

$$J = (\mathbf{a}(\mathbf{X},t)\ \mathbf{p}(\mathbf{X},t) - \mathbf{D})\ \mathbf{W}(\mathbf{X},\mathbf{t})\ (\mathbf{a}(\mathbf{X},t)\ \mathbf{p}(\mathbf{X},t) - \mathbf{D}) \tag{2}$$

with respect to the unknown coefficients that finally yields the approximation

$$\begin{aligned}\mathbf{u}^h(\mathbf{X},t) &= \mathbf{N}(\mathbf{X},t)\ \mathbf{D}(t)\\ \mathbf{N} &= \mathbf{p}(\mathbf{X}_I,t)^T\mathbf{A}(\mathbf{X},t)^{-1}\ \mathbf{G}(\mathbf{X}_I,t)\\ \mathbf{A} &= \mathbf{p}(\mathbf{X}_I,t)\ \mathbf{p}^T(\mathbf{X}_I,t)\ \mathbf{W}(\mathbf{X},\mathbf{t})\\ \mathbf{G}(\mathbf{X}_I,t) &= \mathbf{p}^T(\mathbf{X}_I,t)\ \mathbf{W}(\mathbf{X},\mathbf{t})\end{aligned} \tag{3}$$

where $\mathbf{D}$ indicate nodal parameters, $\mathbf{W}(\mathbf{X},\mathbf{t})$ is a diagonal matrix that contains the weighting functions w; we use the cubic B-spline. We would like to emphasize that an updated Lagrangian kernel is used. Therefore, the reference configuration is updated every n-th time step; n was chosen between 50 and 100 in our simulations. Hence, the material coordinates $\mathbf{X}$ refer not to the initial configuration but to the updated reference configuration. More details can be found for example in [40,85].

In our coupled thermo-mechanical model, we also discretize the temperature field $T(\mathbf{X},t)$ with EFG-shape functions:

$$T^h(\mathbf{X},t) = \mathbf{N}(\mathbf{X},t)\ \mathbf{T}_t \tag{4}$$

where $\mathbf{T}(t)$ is the vector that contains the nodal parameters associated to the temperature field.

In the Smoothed Finite Element Method (SFEM), the compatible strains are replaced by so-called smoothed strains:

$$\tilde{\epsilon}_{ij}(\mathbf{x}^C) = \int_{\Omega_C} \epsilon_{ij}\,\Psi(\mathbf{x}-\mathbf{x}^C)\ d\Omega \tag{5}$$

$\Psi(\mathbf{x}-\mathbf{x}^C)$ denoting a smoothing function that has to obey the following rules:

$$\Psi(\mathbf{x}-\mathbf{x}^C) \geqslant 0, \quad \int_\Omega \Psi(\mathbf{x}-\mathbf{x}^C)\ d\Omega = 1 \tag{6}$$

The key idea of SFEM is to construct smoothing domains as shown in Fig. 1. The integration is done along the boundaries of these smoothing domains Ω_C. There are different ways to construct the smoothing cells and we found the most robust method is based on 2 so-called sub-cells as illustrated in Fig. 1. Choosing a constant smoothing function

$$\Psi(\mathbf{x}-\mathbf{x}^C) = \begin{cases} \frac{1}{A^C} & \mathbf{x}\in\Omega^C \\ 0 & \text{elsewhere}\end{cases}$$

where $A^C = \int_{\Omega^C} d\Omega$ denotes the area of the smoothing domain, the smoothing function can be taken out of the integral in Eq. (5). The volume integral can then be transformed into a boundary integral by the Gauss divergence theorem yielding

$$\tilde{\epsilon}_{ij}(\mathbf{x}^C) = \frac{1}{A^C}\int_{\Gamma^C} \left(u_i n_j\right)^S\ d\Gamma \tag{7}$$

the superscript S indicates symmetric term and $\mathbf{n}$ denotes the normal vector of a smoothing side. The strain field

$$\tilde{\epsilon}_{ij}(\mathbf{x}^C) = \sum_{I=1}^{N} \tilde{\mathbf{B}}_I(\mathbf{x}^C)\mathbf{d}_I \tag{8}$$

in SFEM depends now only on the shape functions themselves and not their derivatives:

$$\tilde{\mathbf{B}}_I(\mathbf{x}^C) = \begin{bmatrix} \tilde{b}_{I1}(\mathbf{x}^C) & 0 \\ 0 & \tilde{b}_{I2}(\mathbf{x}^C) \\ \tilde{b}_{I2}(\mathbf{x}^C) & \tilde{b}_{I1}(\mathbf{x}^C)\end{bmatrix} \tag{9}$$

and

$$\tilde{\mathbf{b}}_I(\mathbf{x}^C) = \frac{1}{A^C}\int_{\Gamma^C} N_I(\mathbf{x})\mathbf{n}(\mathbf{x})\ d\Gamma \tag{10}$$

Moreover, they are evaluated in the physical space and integration is performed along the smoothing sides making them insensitive to mesh distortion. Only one quadrature point is needed to exactly evaluate the integrals for 3-node triangles and 4-node quadrilaterals:

$$\tilde{\mathbf{b}}_I(\mathbf{x}^C) = \sum_{J=1}^{M} N_I(\mathbf{x}_J)\mathbf{n}_J^C l_J^C \tag{11}$$

$\mathbf{x}_J$ denotes the position of the quadrature point at the boundary segment on $\Gamma_J^C; l_J^C$ and $\mathbf{n}_J^C$ indicate their length and normal, respectively.

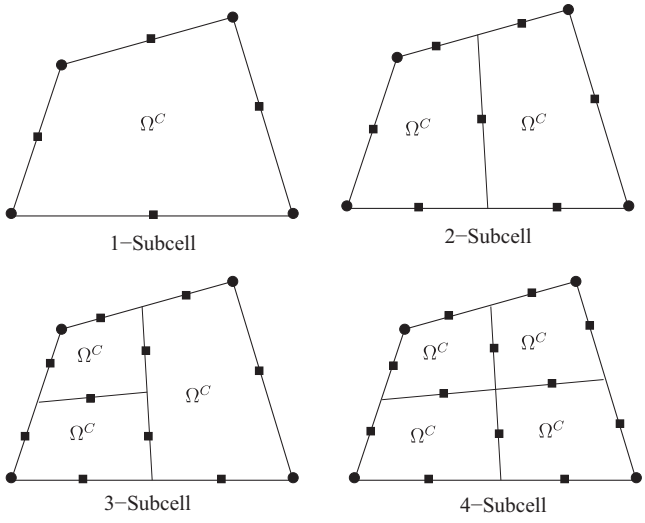

Fig. 1. Subcells for an smoothed finite element; circular dots denote FE nodes and square shaped dots denote quadrature points located at the line segments of the subcells.